



PERGAMON

Deep-Sea Research II 48 (2001) 2227–2239

DEEP-SEA RESEARCH
PART II

www.elsevier.com/locate/dsr2

Long-term (1977–1997) measurements of carbon dioxide in the Eastern North Atlantic: evaluation of anthropogenic input

Aida F. Ríos*, Fiz F. Pérez, F. Fraga

Instituto de Investigaciones Mariñas (CSIC), Eduardo Cabello 6, 36208-Vigo, Spain

Abstract

From 1977 to 1997 CO₂ parameters were measured in the Eastern North Atlantic Ocean. A data set of 12 cruises carried out between 37°N and 47°N, 20°W and the Iberian Peninsula coast, were used to estimate the anthropogenic carbon (C_{ANT}) based on a back-calculation technique, with the aim of evaluating its temporal evolution in that 20-year period. The rate of change of the integrated C_{ANT} down to 2000 m was 0.95 mol m⁻² yr⁻¹. Half of this input corresponds to a direct uptake of atmospheric CO₂ (0.48 mol m⁻² yr⁻¹), while the other half enters by advection. The C_{ANT} advected by the Mediterranean Water (MW) is the most important contributor to the total C_{ANT} advected into the area, representing 59% (0.27 ± 0.09 mol m⁻² yr⁻¹), whereas the Labrador Sea Water contributes only 15% (0.07 ± 0.04 mol m⁻² yr⁻¹). The particular formation mechanism of MW explains its high content of advected C_{ANT}. When MW is formed in the Gulf of Cádiz, 85% of Central Water is entrained by sinking of the Mediterranean Overflow Water. Central Waters have about 50 μmol kg⁻¹ of C_{ANT}; thus this entrainment represents 0.07 GtC yr⁻¹, which is about 26% of the C_{ANT} transported by the thermohaline circulation in the North Atlantic. © 2001 Elsevier Science Ltd. All rights reserved.

1. Introduction

About one-third to one-half of the anthropogenic CO₂ emitted to the atmosphere is taken up by the oceans (Siegenthaler and Sarmiento, 1993); among them, the Atlantic Ocean is considered as the most important CO₂ sink (Sarmiento et al., 1995). Therefore, it is important to improve the knowledge of the uptake of carbon in different provinces to understand and evaluate the global carbon cycle. Several estimates of the anthropogenic carbon uptake have been performed in the North Atlantic using historical data sets such as GEOSECS or TTO (Chen and Millero, 1979;

* Corresponding author.

E-mail address: aida@iim.csic.es (A.F. Ríos).

Chen, 1982; Gruber, 1998). Recently, other estimates have been made from cruises that took place in the 1990s (Körtzinger et al., 1998; Wanninkhof et al., 1999). Here, we use a set of 12 cruises from the eastern North Atlantic between 1977 and 1997, with the aim of evaluating the temporal evolution during these 20 years of the anthropogenic CO₂ input in the eastern North Atlantic.

2. Database

Temperature, salinity, oxygen, nutrients, alkalinity and dissolved inorganic carbon data from different cruises were used to estimate the anthropogenic carbon based on a back-calculation technique. Table 1 shows the characteristics of the 12 cruises; station locations of the cruises are shown in the map (Fig. 1). The dissolved inorganic carbon (C_T) was estimated from measured pH and alkalinity (TA) using the thermodynamic equations of the carbonate system (Dickson, 1981), with the dissociation constants of Mehrbach et al. (1973), in all cruises, except for the TTO and OACES cruises. TTO C_T data were calculated from potentiometric C_T and alkalinity. For the OACES cruise, the C_T measurements were performed using coulometric detection with a single operator multi-parameter metabolic analyzer (SOMMA) inlet system (Johnson et al., 1993).

TA was determined by potentiometric titration methods as described in Pérez and Fraga (1987a). Likewise, pH was measured potentiometrically in NBS scale (Pérez and Fraga, 1987b) in “Galicia’s”, VIVALDI, Bord-Est 3 and MORENA I cruises, while pH was determined spectrophotometrically in the OACES and FOUREX cruises (Clayton and Byrne, 1993). A comprehensive description of the cruise, the sampling procedures, and the analytical techniques have been discussed in Manríquez et al. (1978), Fraga et al. (1978), Mouriño et al. (1984), Pérez et al. (1985), Fraga et al. (1985), Mouriño et al. (1985), Fraga et al. (1987), Griffiths et al. (1992), Castle et al. (1998) and Bacon (1998).

Table 1

Characteristics of the 12 cruises. The different stations sampled in each cruise are represented by the same symbols in Fig. 1^a

Symbol	Year	Month	Cruise	pH	TA	C _T
◇	1977	October	Galicia IV	P	P	Cal
▲	1981	November	TTO	—	P	P
▼	1982	November	Galicia V	P	P	Cal
△	1983	December	Galicia VI	P	P	Cal
●	1984	February	Galicia VII	P	P	Cal
□	1984	July	Galicia VIII	P	P	Cal
○	1986	September	Galicia IX	P	P	Cal
■	1989	May	Bordest 3	P	P	Cal
◆	1991	April–May	Vivaldi	P	P	Cal
▽	1993	May	Morena I	P	P	Cal
+	1993	July	OACES	S	P	Coul
×	1997	August	Fourex	S	P	Cal

^aTA is total alkalinity, C_T is total inorganic carbon, P means Potentiometric, S spectrophotometric, Coul coulometric, M measured, and Cal calculated.

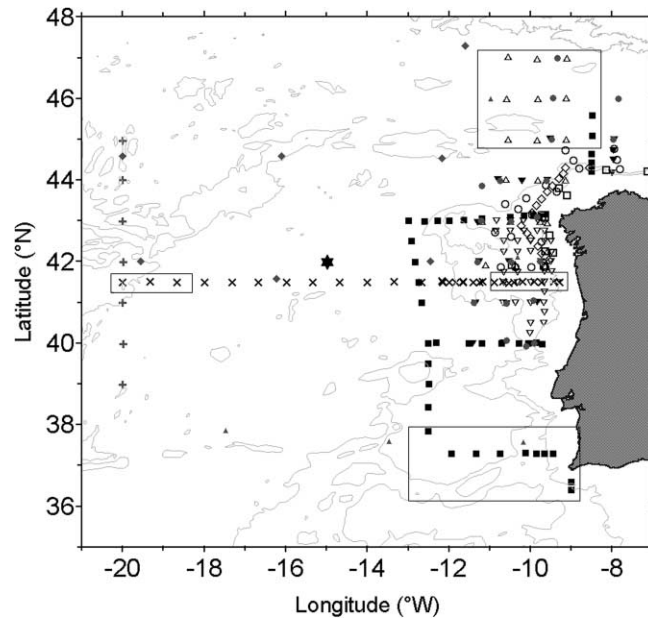


Fig. 1. Map of the sampled area. The locations of the stations are indicated by different symbols according to the cruise as given in Table 1. The squares show the clusters of stations used to obtain the vertical profiles Northwards at 46°N, Southwards at 38°N, Eastwards at 10°W and Westwards at 20°W. The star indicates the central position of reference (42°N, 15°W).

The previous potentiometric methodologies were validated in the WOCE sections A17 and A14 in the South Atlantic where a comparative experiment was performed (Ríos and Pérez, 1999). Analytical errors were ± 0.003 in pH and $\pm 1.1 \mu\text{mol kg}^{-1}$ in TA based on 61 replicates. The average difference between calculated and measured C_T was as low as $0.2 \pm 3.0 \mu\text{mol kg}^{-1}$ for 964 couples. Calculated C_T for 76 certified reference materials (CRMs) also agreed very well with certified concentrations. Finally, the average difference of the 10 C_T samples measured at the Scripps Institution of Oceanography calculated from pH and TA was only $0.9 \pm 2.6 \mu\text{mol kg}^{-1}$. For the cruises performed before 1994, substandard seawater was used to ensure the internal consistency in each cruise. This substandard seawater, similar to CRM, is “quasi-steady” surface seawater, which was filtered and stored in 25-l plastic containers. To avoid the long-term bias, a quality control based on a steady state for deep waters in the relationship pH versus nitrate, and TA normalized to salinity 35 versus silicate was made (Ríos and Pérez, 1999).

3. Method

The initial concentrations of the CO_2 in source regions of different water masses are modified by the oxidation of organic materials and the dissolution of carbonaceous skeletons (Broecker and Peng, 1982; Takahashi et al., 1985; Anderson and Sarmiento, 1994). In addition, the initial CO_2 of any water mass depends on the CO_2 levels in the overlying atmosphere, which have increased from

the pre-industrial reference value of 278 ppm. The total amount of anthropogenic CO₂ dissolved in the ocean can be estimated assuming that: (1) dissolved oxygen and CO₂ are close to equilibrium (or with the same disequilibrium) with the atmosphere during water-mass formation; and (2) alkalinity is not significantly affected by the CO₂ increase (e.g. Chen and Millero, 1979; Poisson and Chen, 1987; Gruber et al., 1996). The anthropogenic CO₂ (C_{ANT}) was calculated from C_T, TA and dissolved oxygen measured at the sea:

$$C_{ANT} = C_T - AOU/R_C - 1/2(TA - TA^0 + AOU/R_N) - C_{T278}^0,$$

where AOU/R_C is the C_T increase by organic matter oxidation. Apparent oxygen utilisation (AOU), is calculated with the oxygen saturation equation of Benson and Krause (UNESCO, 1986). R_C is a stoichiometric coefficient (= -ΔO₂/ΔC). In addition, 1/2(ΔTA + AOU/R_N) is the C_T change due to CaCO₃ dissolution in deep-ocean waters (Broecker and Peng, 1982), where ΔTA is the total alkalinity change from the initial value during water mass formation (TA⁰), and R_N is a second stoichiometric coefficient (= -ΔO₂/ΔN). For open-ocean waters below 400 m, R_C = 1.45 and R_N = 10.6 (Anderson and Sarmiento, 1994). TA⁰ stands for preformed alkalinity and was calculated from salinity and 'PO' using the empirical equation of Gruber et al. (1996): TA⁰ = 367.5 + 54.9S + 0.074'PO', where 'PO' = O₂ + R_PPO₄. R_P is a stoichiometric coefficient (= -ΔO₂/ΔP), with a constant value of 170 molO₂ molP⁻¹ (Anderson and Sarmiento, 1994). C_{T278}⁰ is the initial C_T of any water mass in the pre-industrial era, which can be calculated from time-independent TA⁰ and the atmospheric pCO₂ level at that time and water vapour pressure (Pérez et al., submitted), where pCO₂ = xCO₂⁰ · (P_{atm}-vapor pressure) according to DOE (1994). The mole fraction of CO₂ in the pre-industrial atmosphere (xCO₂⁰) was 278.2 ppm (Neftel et al., 1994; Sarmiento et al., 1995).

Previous approaches have been used by other authors to calculate C_{ANT} (Chen and Pytkowicz, 1979; Chen, 1982, 1993; Poisson and Chen, 1987; Gruber et al., 1996; Körtzinger et al., 1998). Gruber et al. (1996) introduced the disequilibrium term, which includes the CO₂ disequilibrium at the time the water lost contact with the atmosphere plus any residual effects due to their choice of oxygen and alkalinity end-members and data uncertainties. Available CFC data for thermocline waters of two cruises enabled the estimation of the disequilibrium term. The calculated values (3.8 ± 4.8 μmol kg⁻¹) notably differed from those reported by Gruber et al. (1996) for the North Atlantic (between -12 and -24 μmol kg⁻¹), but agreed with the estimations obtained by Pérez et al. (submitted). Furthermore, considering the assumptions made by Gruber et al. (1996) that the ocean has been operating in a steady state, the effective disequilibrium would have been practically constant, and therefore would not effectively affect our results, since we are dealing with temporal changes of C_{ANT}.

The method to estimate C_{ANT} is subject to a number of uncertainties. The maximum errors estimated by other authors range between ± 6 μmol kg⁻¹ (Sabine et al., 1999) and ± 10 μmol kg⁻¹ (Gruber et al., 1996; Körtzinger et al., 1998). We have performed the same error analysis, obtaining ± 10.3 μmol kg⁻¹. But as our study is based on an average C_{ANT} profile for each cruise, the terms and variables involved in the calculations are so many that the averaging effect acting on the independent errors becomes large enough to decrease considerably the real errors (Matsukawa and Suzuki, 1985). Deep waters below 3000 db are expected to have no C_{ANT} due to their old age (Körtzinger et al., 1998). Below 3000 db the C_{ANT} average value and standard deviation obtained for the whole data set was 0.7 ± 2.5 μmol/kg (n = 274). Given that the

data population has no C_{ANT} (the shift 0.7 is not significant), the standard deviation of C_{ANT} below 3000 db equivalent to the error estimate of C_{ANT} . Therefore, the error of the C_{ANT} estimates is $\pm 2.5 \mu\text{mol/kg}$.

4. Results

The C_{ANT} was calculated for the entire temporal set of stations. Then, in order to obtain a vertical profile for each cruise, individual station values were linearly interpolated to fixed depth levels, then for each cruise an average C_{ANT} profile was obtained (Fig. 2). The highest C_{ANT} values appear in the main thermocline down to about 600 db, with a range between 33 and 50 $\mu\text{mol kg}^{-1}$. Below this level the C_{ANT} values decrease slowly down to 1200 db, exhibiting values varying from 25 to 38 $\mu\text{mol kg}^{-1}$. Beneath 1200 db, C_{ANT} values decrease quickly, reaching values lower than 5 $\mu\text{mol kg}^{-1}$ at 3000 db. The deep waters show the lowest C_{ANT} concentrations (-3 to 3 $\mu\text{mol kg}^{-1}$). Down to 2000 db, the slopes of the C_{ANT} profiles differ in relation with the surveyed area. The cruises performed westward from 15°W, such as VIVALDI, OACES and FOUREX, present slopes higher than cruises carried out farther east and south. Therefore, it seems to be a spatial component in the variability of the average C_{ANT} profiles.

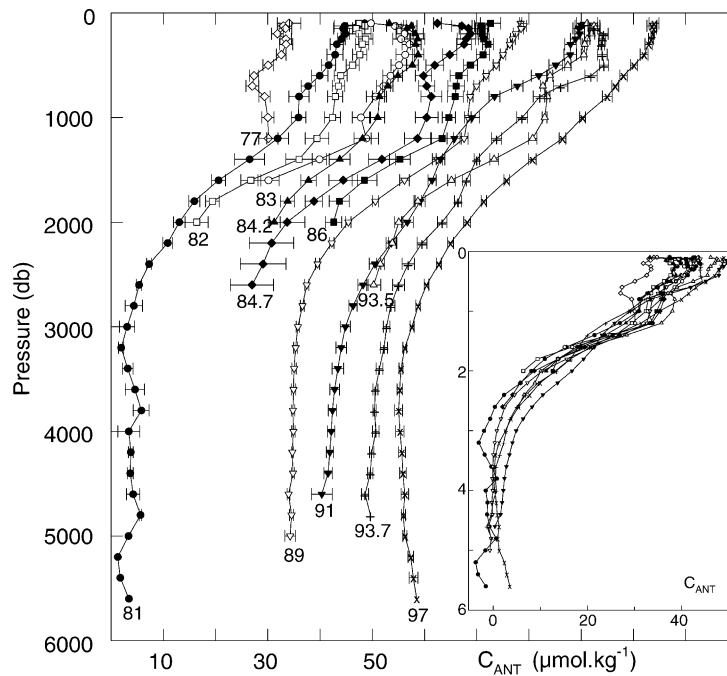


Fig. 2. Average vertical profile of C_{ANT} for each cruise. The same set of symbols is used in Table 1 and Fig. 1. Each profile is displaced $5 \mu\text{mol kg}^{-1}$. The error bar represents the SDM (standard deviation weighted by the number of individual determinations). The year the cruise was performed is detailed at the extreme of each profile. When two cruises were performed in the same year, the month is indicated next to the year separated by one point. The inset shows the average profiles represented with the same scale.

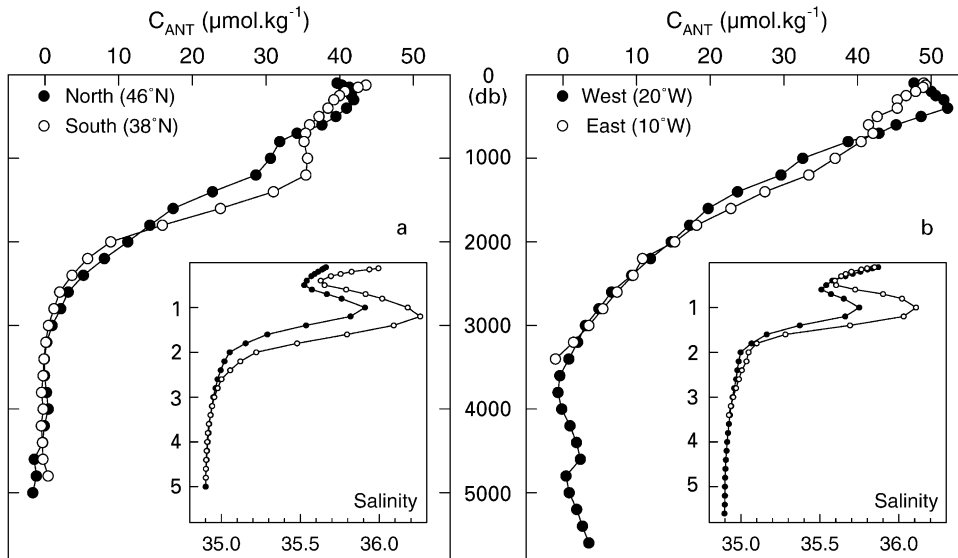


Fig. 3. Average vertical profiles of C_{ANT} in $\mu\text{mol.kg}^{-1}$ for the (a) Northern 46°N (black circles) and Southern 38°N (open circles); (b) Western 20°W (black circles) and Eastern 10°W (open circles) positions. Average vertical profiles of salinity for the same locations are included in the corresponding insets.

Even taking into consideration this variability due to the average position of each cruise, the gradual temporal increase of C_{ANT} concentrations over the main thermocline is evident. Starting from $30\ \mu\text{mol.kg}^{-1}$ in 1977 (Galicia IV), going through $40\ \mu\text{mol.kg}^{-1}$ in 1981 (TTO), reaching concentrations between 40 and $45\ \mu\text{mol.kg}^{-1}$ in the 1980s, and finally rising from 46 to $50\ \mu\text{mol.kg}^{-1}$ in the 1990s. Conversely, in deep layers (below $2000\ \text{db}$), although C_{ANT} seems to increase with time (Fig. 2), the average C_{ANT} values ($2 \pm 3\ \mu\text{mol.kg}^{-1}$) are rather constant and within the error of the model.

The entire set of cruises did not have the same spatial coverage. Thus, the average thermohaline profiles of each cruise differ spatially, and therefore the percentage of water masses is also different, introducing variations in the C_{ANT} inventory. To remove this effect on the average C_{ANT} profiles, we have obtained average vertical profiles of C_{ANT} for four locations North at 46°N , South at 38°N , East at 10°W , and West at 20°W . The C_{ANT} average vertical profiles at the northern and southern positions (Fig. 3a) were obtained from the Galicia VI, VII and Bord-Est 3 data. In the upper $700\ \text{db}$, the C_{ANT} values are slightly higher at the northern than at the southern position. This layer belongs to the Central Water domain. Thereby, the differences found in C_{ANT} and salinity depend on the origin of the Eastern North Atlantic Central Water, subpolar or subtropical (Ríos et al., 1992). Between 700 and $1400\ \text{db}$ the influence of the Mediterranean Water (MW) is higher at the southern position, whereas the northern profile is more influenced by Labrador Sea Water (LSW). Similarly, we have calculated the mean vertical C_{ANT} profiles for the W–E positions from the FOUREX data (Fig. 3b). Within the upper $700\ \text{db}$, the Central Waters domain, the C_{ANT} concentrations are higher at the western than at the eastern position. Between 1000 and $2000\ \text{db}$ the MW influence predominates towards the east, while the LSW influence is higher towards the west. Along the N–S

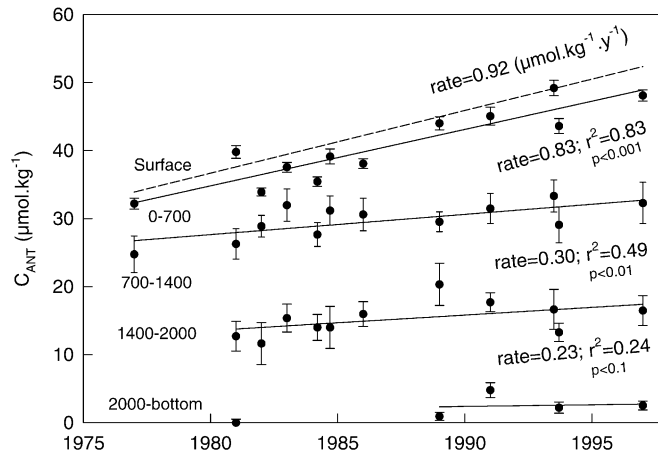


Fig. 4. Temporal evolution of the integrated C_{ANT} within the four depth intervals: Note that C_{ANT} concentrations were previously normalised to the average position, 42°N , 15°W . The annual rate of C_{ANT} increase ($\mu\text{mol kg}^{-1} \text{yr}^{-1}$) along with its determination coefficient is given for each later. The dashed line is the surface annual rate assuming equilibration with the atmospheric $p\text{CO}_2$ increase in the zone. The error bar represents the SDM (standard deviation weighted by the number of individual determinations).

and W–E axes, the anomalies of C_{ANT} concentrations are remarkably related with the salinity anomalies, which indicate the spreading of MW and LSW.

In order to obtain a spatially normalised average profile of C_{ANT} for every cruise, we have calculated the average profile of salinity for the central position of the study area (42°N , 15°W) using data from the FOUREX cruise. Then, we have normalised the C_{ANT} average profile of each cruise by the ratio between salinity and C_{ANT} anomalies, in such a way that every C_{ANT} profile is representative of the same position (42°N , 15°W) (see Appendix A).

We have divided the water column into four layers according to the spreading domain of the different water masses of the study region. Central Waters occupy the upper layer. MW spreads from 700 to 1400 db. The third layer between 1400 and 2000 db comprises the core of LSW. Deep and bottom waters occupy the layer up to 2000 db. Using the C_{ANT} profiles normalised to the centre of the study area, we have averaged C_{ANT} values within the previous depth layers, searching for any temporal evolution in the C_{ANT} inventory in the Eastern North Atlantic.

Fig. 4 shows the annual rates of C_{ANT} invasion within each layer, as well as the determination coefficient for every trend line. The upper layer shows an annual C_{ANT} uptake rate of $0.83 \mu\text{mol kg}^{-1} \text{yr}^{-1}$ in agreement with the surface annual rate of $0.92 \mu\text{mol kg}^{-1} \text{yr}^{-1}$. This latter value was estimated assuming equilibrium between the upper mixed layer (< 150 db) and the atmospheric $p\text{CO}_2$ increase in the zone, reported by the monitoring station for atmospheric $p\text{CO}_2$ of Izaña (Tenerife, Spain). Note the gradual but remarkable decrease of the C_{ANT} annual rates between the domain of MW and LSW, 0.30 and $0.23 \mu\text{mol kg}^{-1} \text{yr}^{-1}$, respectively. The deep-water layer does not present any discernible C_{ANT} annual rate; the average C_{ANT} content is $1.9 \pm 2.0 \mu\text{mol kg}^{-1}$.

The average C_{ANT} inventory for the upper 2000 m is $0.95 \text{ mol m}^{-2} \text{yr}^{-1}$. Considering an average upper mixed layer of 500 m in the study zone (Paillet and Arhan, 1996; Pollard et al., 1996) and the

Table 2

Mass transport, in Sverdrup ($1 \text{ Sv} = 10^6 \text{ m}^3 \text{ s}^{-1}$), through the three walls of the box comprised within 37°N – 47°N , 20°W and the Iberian Peninsula coast. Transports, with an error estimate $\pm 30\%$, were taken from Saunders (1982). Positive transport values indicate fluxes into the box, conversely negative values indicate outflows. 1990-referred concentrations of C_{ANT} for the different layers were calculated according to the annual rates of C_{ANT} increase given in Fig. 4. Advected C_{ANT} rates were calculated by multiplying the transports by the previous C_{ANT} concentrations. The errors of the advected C_{ANT} and total C_{ANT} storage rates were calculated from an error propagation analysis, including the transport and the C_{ANT} estimation errors

Box layers	Transport (Sv) (Saunders, 1982)			C_{ANT} ($\mu\text{mol kg}^{-1}$) for 1990			Advected C_{ANT} rates	Total C_{ANT} storage rates
	N	S	W	N	S	W		
Pressure (db)							$\text{mmol m}^{-3} \text{ yr}^{-1}$	$\text{mmol m}^{-3} \text{ yr}^{-1}$
0–700	– 1	– 4.5	+ 5.5	44	42	43	0.18 ± 0.05	0.85 ± 0.12
700–1400	– 2.5	+ 2	+ 0.5	31	36	29	0.39 ± 0.13	0.31 ± 0.10
1400–2000	+ 6	– 2	– 4	16	18	14	0.12 ± 0.07	0.23 ± 0.13

input of CO_2 across the surface layer ($0.92 \mu\text{mol kg}^{-1} \text{ yr}^{-1}$), the atmospheric input of C_{ANT} is $0.47 \text{ mol m}^{-2} \text{ yr}^{-1}$, which represents a 49% of the estimated inventory. The likely mechanism responsible for this accumulation is an advection of C_{ANT} -loaded water driven by the thermohaline circulation.

To investigate the portion of C_{ANT} advected into the study zone, we have defined a box comprised within 37°N , 47°N , 20°W and the coast. This box has three layers, coinciding with the Central Waters, MW and LSW domains as defined previously (see Table 2). The volume transports across the box walls and within each layer were taken from Saunders (1982). The corresponding C_{ANT} concentrations are referred to the year 1990 according to the annual rates of C_{ANT} increase given in Fig. 4. Then, as these values represent an average spatial mean for the central position (42°N , 15°W), we have applied the corresponding geographical water masses correction, using salinity, to obtain values referred to the actual position of the walls. The C_{ANT} -advected rates at each layer were obtained by subtracting the inflows by the outflows into the box.

Table 2 shows the advected and storage rates of C_{ANT} . In the Central Water layer, the advection rate ($0.18 \text{ mmol m}^{-3} \text{ yr}^{-1}$) only contributes with a 21% to the storage rate of C_{ANT} ($0.85 \text{ mmol m}^{-3} \text{ yr}^{-1}$). Thus, the remaining 79% is the atmospheric C_{ANT} ($0.67 \text{ mmol m}^{-3} \text{ yr}^{-1}$) that penetrates through the air-sea interface into the box. In the layer dominated by MW, all the C_{ANT} is advected into the box. Moreover, the C_{ANT} storage rate ($0.31 \text{ mmol m}^{-3} \text{ yr}^{-1}$) is even $0.08 \text{ mmol m}^{-3} \text{ yr}^{-1}$ lower than the advected C_{ANT} rate, suggesting that MW is losing C_{ANT} , probably by mixing with LSW. In the LSW domain the C_{ANT} advected ($0.12 \text{ mmol m}^{-3} \text{ yr}^{-1}$) by this water mass is half of the storage rate. Therefore, the remaining C_{ANT} ($0.11 \text{ mmol m}^{-3} \text{ yr}^{-1}$) must come from the above MW layer by mixing.

5. Discussion

Both the average vertical profiles (Fig. 2) and the depth-averaged values geographically normalised (Fig. 4) point to a temporal increase in the C_{ANT} content in the eastern North Atlantic. In

the upper 700 db layer, the Central Water domain, the annual rate of C_{ANT} -uptake ($0.83 \mu\text{mol kg}^{-1} \text{yr}^{-1}$) agrees with the surface annual rate ($0.92 \mu\text{mol kg}^{-1} \text{yr}^{-1}$), calculated from the atmospheric $p\text{CO}_2$ increase in the study zone assuming atmospheric equilibrium within the upper 150 m. The annual rates of C_{ANT} -uptake decrease with depth in the layers dominated by MW and LSW (0.30 and $0.23 \mu\text{mol kg}^{-1} \text{yr}^{-1}$, respectively). No C_{ANT} annual rate was found in the deep layer (2000 db-bottom). In this layer the average C_{ANT} concentration for the whole the period and cruises was $1.9 \pm 2.0 \mu\text{mol kg}^{-1}$. This value is within the range of uncertainty of the method for estimating anthropogenic carbon.

The annual rate of C_{ANT} -uptake in the upper layer seems to keep pace with the atmospheric $p\text{CO}_2$ increase. However, if we integrate the C_{ANT} concentrations down to 2000 m, we obtain the same inventory ($0.95 \text{mol m}^{-2} \text{yr}^{-1}$) as if considering an atmospheric-equilibrated upper mixed layer 1000 m deep. However, according to Paillet and Arhan (1996) and Pollard et al. (1996), the upper mixed layer or “annually ventilated” layer in this area comprises about the upper 500 m, being deeper (~ 700 m) north of 42°N and shallower (~ 200 m) south of 41°N . Consequently, the total uptake rates of C_{ANT} have a portion of C_{ANT} accumulated by advection through thermohaline circulation.

Combining data from different cruises for a temporal-series analysis references a good quality control check in order to avoid systematic offsets in the several databases. We have addressed this point in the Database and Method sections. However, we would like to emphasise the consistency of our analysis and results; both the obtained rate of C_{ANT} -uptake in the upper mixed layer and the mean values of C_{ANT} below 2000 db lead us to consider our data set as suitable and consistent for estimating the C_{ANT} inventory in the eastern North Atlantic Ocean. Another source of error could be the spatial normalisation, we have estimated it to be lower than $0.5 \mu\text{mol kg}^{-1}$ as explained in Appendix A. The highest errors in this study come from the estimation of the advection rates, and are mainly ascribed to the 30% error in the volume fluxes. A propagation error analysis for the advected C_{ANT} rates was also carried out (Table 2).

The examination of the C_{ANT} rates (Table 2) within depth intervals showed for the upper layer (0–700 db) a C_{ANT} advection rate of $0.12 \text{mol m}^{-2} \text{yr}^{-1}$, and therefore, an atmospheric C_{ANT} -uptake rate of $0.47 \text{mol m}^{-2} \text{yr}^{-1}$. This rate is exactly the same if considering an average upper mixed layer of 500 m (Pollard et al., 1996; Paillet and Arhan, 1996) keeping pace with the $p\text{CO}_2$ increase in the atmosphere. Besides, this net C_{ANT} -uptake rate is similar to the net CO_2 flux across the air–sea interface of $0.44 \text{mol m}^{-2} \text{yr}^{-1}$ on the North Atlantic for the 0– 40°N latitude interval given by Roos and Gravenhorst (1984). Takahashi et al. (1999) gave combined flux of natural and anthropogenic CO_2 of $2 \text{mol m}^{-2} \text{yr}^{-1}$ for the area 38– 46°N by 10– 20°W .

The results given in Table 2 show that half of the entry of C_{ANT} in the study area corresponds to a direct uptake of atmospheric CO_2 ($0.48 \text{mol m}^{-2} \text{yr}^{-1}$). The other half enters the box by advection. Contrary to expectations, the C_{ANT} advected by MW is the most important input of advected C_{ANT} in the area, contributing 59% ($0.27 \text{mol m}^{-2} \text{yr}^{-1}$) of the total advected C_{ANT} , while the LSW contributes only 15% ($0.07 \text{mol m}^{-2} \text{yr}^{-1}$). According to Cunningham and Haine (1995), the LSW core in our study area estimated by CFC data is about 15 years old. MW is an older water mass, with a residence time in the Mediterranean Sea of about 70 years (Pickard and Emery, 1990); presumably, LSW should be loaded with a higher C_{ANT} content, which it is advected into our area.

The formation mechanism of MW explains its high content of advected C_{ANT} . Mediterranean overflow water (MOW) with 38.4 salinity enters the North Atlantic, dragging down Central Waters

salinities to around 35.7, sinking until reaching the appropriate density level, forming MW with 36.2 final salinity. According to Bryden et al. (1994), 0.78 Sv of Central Water flow into the Mediterranean Sea through the Strait of Gibraltar, and 0.67 Sv are exported out as MOW. Slater and Bryden (2000), in a 3-sided box around the Gulf of Cadiz, found a net outflow from the box in the MW depth range of about 4.4 Sv. We calculate the amount of entrained Central Water as 3.73 Sv. This value is within the range estimated by Mazé et al. (1997), 3–4 Sv, and by Rhein and Hinrichsen (1993), 3.6 Sv using CFC and nutrient data. Therefore, MW is composed of 85% Central Water and 15% MOW. A small portion of Central Water also penetrates through the Strait of Gibraltar at the Mediterranean Sea where deep water is formed in the Levantine zone and Lion Gulf.

The downward entrainment of upper water in the Gulf of Cadiz is a particular mechanism contributing to the eastern boundary ventilation (Pedlosky, 1983; Arhan et al., 1994). According to this mechanism and considering a current C_{ANT} concentration of about $50 \mu\text{mol kg}^{-1}$, we obtain that $0.07 \text{ Gt C yr}^{-1}$ of Central Waters are draw down to form MW. Although this rate seems to be small, it represents 26% of the rate of the C_{ANT} transported by the thermohaline circulation in the North Atlantic, considering a transport of 14 Sv (Schmitz, 1996) in the North Atlantic. In summary, our results demonstrate that the C_{ANT} sequestered by MW through the downward entrainment of Central Water is sufficiently important to be considered in the global carbon budgets and in models of oceanic circulation.

Acknowledgements

This work was supported by grant number CICYT MAR97-0660. The authors wish to thank all the participants in the 12 cruises and to Marta Álvarez for her comments and English correction, as well as Trinidad Rellán for the management of the figures. We thank Dr. Wolfgang Koeve and an anonymous reviewer for their valuable suggestions and comments on an earlier version of this paper.

Appendix A. Spatially normalisation of the C_{ANT} average profiles

In order to normalise the C_{ANT} average profiles spatially for each cruise to the same central position (42°N , 15°W), we first “moved” each profile to the central position using the latitude and longitude differences between each profile (i) and the reference point (r). Then, the corresponding C_{ANT} anomaly (ΔC_{ANT}) was calculated from salinity differences (ΔS) between the profile and the central point in the North–South and West–East directions. In order to do this a $\Delta C_{ANT}/\Delta S$ regression line was calculated by depth intervals and N–S, W–E directions (Table 3):

$$\Delta C_{ANT} = [(\Delta C_{ANT(LONG)} \cdot \Delta \text{Long}_{(i-r)}) + (\Delta C_{ANT(LAT)} \cdot \Delta \text{Lat}_{(i-r)})] / (\Delta \text{Long}_{(i-r)} + \Delta \text{Lat}_{(i-r)}),$$

$$\text{where } \Delta C_{ANT(LONG)} = (S_i - S_r) [\Delta C_{ANT(W-E)} / \Delta S_{(W-E)}]$$

$$\text{and } \Delta C_{ANT(LAT)} = (S_i - S_r) [\Delta C_{ANT(N-S)} / \Delta S_{(N-S)}].$$

Table 3

Slopes and determination coefficients between ΔC_{ANT} and ΔS for the West–East and North–South variation obtained from data showed in Fig. 3

Level (db)	$\Delta C_{\text{ANT(W-E)}} / \Delta S_{\text{(W-E)}}$	R^2 (W-E)	Error of the $\Delta C_{\text{ANT(LONG)}}$ estimate ($\mu\text{mol kg}^{-1}$)	$\Delta C_{\text{ANT(N-S)}} / \Delta S_{\text{(N-S)}}$	r^2 (N-S)	Error of the $\Delta C_{\text{ANT(LAT)}}$ estimate ($\mu\text{mol kg}^{-1}$)
0–700	-66 ± 34	0.49	± 1.9	-11.4 ± 0.3	0.97	± 0.05
700–1400	9.6 ± 1.4	0.85	± 0.49	15.3 ± 2.0	0.87	± 0.8
1400–2000	22.4 ± 5.8	0.74	± 0.26	5.8 ± 0.01	0.998	± 0.003

The error on C_{ANT} generated by this normalisation is given by the sum of the relative errors of salinity and the slopes. The salinity analytical error is ± 0.005 , with a relative error of about 0.014%. The maximum north–south and west–east gradients of salinity were 0.38 and 0.35, respectively, which represent errors of 5.3×10^{-5} and 5×10^{-5} psu. Therefore, these errors can be considered as negligible with regard to the error of the slopes. The error of the $\Delta C_{\text{ANT(LONG)}}$ and $\Delta C_{\text{ANT(LAT)}}$ estimates were calculated from the relative error of the slope and the north–south and west–east gradients. These errors are given in Table 3.

References

- Anderson, L.A., Sarmiento, J.L., 1994. Redfield ratios of remineralization determined by nutrient data analysis. *Global Biogeochemical Cycles* 8, 65–80.
- Arhan, M., Colin de Verdière, A., Mémery, L., 1994. The Eastern Boundary of the Subtropical North Atlantic. *Journal of Physical Oceanography* 24, 1296–1316.
- Bacon, S., 1998. RRS Discovery cruise 230, 07-August–17 September 1997. Two hydrographic sections across the boundaries of the Subpolar Gyre: FOUREX. Southampton. Oceanography Centre Cruise Report, No. 16, 104pp.
- Broecker, W.S., Peng, T.-H., 1982. *Tracers in the Sea*. Columbia University, Eldigio Press, New York, 690pp.
- Bryden, H.L., Candela, J., Kinder, T.H., 1994. Exchange through the Strait of Gibraltar. *Progress in Oceanography* 33, 201–248.
- Castle, R., Wanninkhof, R., Doney, S.C., Bullister, J., Johns, L., Feely, R.A., Huss, B.E., Millero, F.J., Lee, K., 1998. Chemical and hydrographic profiles and underway measurements from the North Atlantic during July and August of 1993. NOAA Data Report ERL AOML-32, Springfield NJ, NOAA/AOML.
- Chen, C.T.A., 1982. On the distribution of anthropogenic CO_2 in the Atlantic and Southern oceans. *Deep-Sea Research I* 29, 563–580.
- Chen, C.T.A., 1993. The oceanic anthropogenic CO_2 sink. *Chemosphere* 27, 1041–1064.
- Chen, C.T., Millero, F., 1979. Gradual increase of oceanic CO_2 . *Nature* 277, 205–206.
- Chen, C.T.A., Pytkowicz, R.M., 1979. On the total CO_2 -titration alkalinity–oxygen system in the Pacific ocean. *Nature* 281, 362–365.
- Chapin, T.D., Byrne, R.H., 1993. Spectrophotometric seawater pH measurements: total hydrogen ion concentration scale calibration of m-cresol purple and at-sea results. *Deep-Sea Research I* 40, 2115–2129.
- Cunningham, S.A., Haine, T.W.H., 1995. Labrador sea water in the Eastern North Atlantic. Part I: a synoptic circulation inferred from a minimum in potential vorticity. *Journal of Physical Oceanography* 25, 649–665.
- Dickson, A.G., 1981. An exact definition of total alkalinity and procedure for the estimation of alkalinity and total inorganic carbon from titration data. *Deep-Sea Research* 28, 609–623.

- DOE, 1994. In: Dickson, A.G., Goyet, C. (Eds.), *Handbook of Methods for the Analysis of the Various Parameters of the Carbon dioxide System in Sea Water*; Version 2, unpublished manuscript.
- Fraga, F., Estrada, M., Mouriño, C., 1978. Campaña “Galicia IV”. Datos básicos II. Resultados Expediciones Científicas B/O Cornide 7, 241–256.
- Fraga, F., Figueiras, F.G., Prego, R., Pérez, F.F., Ríos, A.F., 1987. Campaña “Galicia IX”. *Oceánica. Datos Informativos Instituto Investigaciones Marinas* 20, 1–148.
- Fraga, F., Mouriño, C., Pérez, F.F., Ríos, A.F., Marrasé, C., 1985. Campaña “Galicia VII”. Datos básicos. Datos Informativos Instituto Investigaciones Pesqueras 12, 1–50.
- Griffiths, G., Cunningham, S., Griffiths, M., Pollard, R.T., Leach, H., Holley, S., Paylor, R., Haine, T.W.N., Ríos, A., Alderson, S.G., Lowry, R.K., Smith, P., Preston, M., Gwilliam, T.J.P., Smithers, J., Keene, S., Hemmings, J., Anderson, T.R., 1992. CTD oxygen, tracer and nutrient data from RRS Charles Darwin Cruises 58/59 in the NE Atlantic as part of Vivaldi '91. Institute of Oceanographic Sciences Deacon Laboratory, NERC, Report No. 296, 51pp.
- Gruber, N., 1998. Anthropogenic CO₂ in the Atlantic Ocean. *Global Biogeochemical Cycles* 12, 165–191.
- Gruber, N., Sarmiento, J.L., Stocker, T.F., 1996. An improved method for detecting anthropogenic CO₂ in the oceans. *Global Biogeochemical Cycles* 10, 809–837.
- Johnson, K.M., Wills, K.D., Butler, D.B., Johnson, W.K., Wong, C.S., 1993. Coulometric total carbon dioxide analysis for marine studies: maximizing the performance of an automated gas extraction system and coulometric detector. *Marine Chemistry* 44, 167–187.
- Körtzinger, A., Mintrop, L., Duinker, J.C., 1998. On the penetration of anthropogenic CO₂ into the North Atlantic Ocean. *Journal of Geophysical Research* 103, 18 681–18 689.
- Manríquez, M., Mouriño, C., Fraga, F., 1978. Campaña “Galicia IV”. Datos básicos I. Resultados Expediciones Científicas B/O Cornide 7, 195–240.
- Matsukawa, Y., Suzuki, T., 1985. Box model analysis of hydrographic behaviour of nitrogen and phosphorus in a eutrophic estuary. *Journal of Oceanographic Society of Japan* 41, 407–426.
- Mazé, J.P., Arhan, M., Mercier, H., 1997. Volume budget of the eastern boundary layer off the Iberian Peninsula. *Deep-Sea Research I* 44, 1543–1574.
- Mehrbach, C., Culberson, C.H., Hawley, J.E., Pytkowicz, R.M., 1973. Measurement of the apparent dissociation constants of carbonic acid in seawater at atmospheric pressure. *Limnology and Oceanography* 18, 897–907.
- Mouriño, C., Pérez, F.F., Ríos, A.F., Fraga, F.F., 1984. Campaña “Galicia V”. Datos básicos. Datos Informativos Instituto Investigaciones Pesqueras 10, 29–61.
- Mouriño, C., Pérez, F.F., Ríos, A.F., Manríquez, M., Estrada, M., Marrasé, C., Prego, R., Fraga, F., 1985. Campaña “Galicia VIII”. Datos básicos. Datos Informativos Instituto Investigaciones Pesqueras 13, 1–108.
- Neftel, A., Friedli, H., Moor, E., Lötscher, H., Oeschger, H., Siegenthaler, U., Stauffer, B., 1994. Historical CO₂ record from the Siple station ice core. In: Boden T., Kaiser D., Sepanski R., Stoss F. (Eds), *In Trends'93: A Compendium of Data on Global Change*, Report. ORNL/CDIAC-65, pp. 11–14. (Carbon dioxide Inf. Anal. Cent., Oak Ridge Natl. Lab., Oak Ridge Tenn.)
- Paillet, J., Arhan, M., 1996. Shallow Pycnoclines and Mode Water Subduction in the Eastern North Atlantic. *Journal of Physical Oceanography* 26, 96–114.
- Pedlosky, J., 1983. Eastern boundary ventilation and the structure of the thermohaline. *Journal of Physical Oceanography* 13, 2038–2044.
- Pickard, G.L., Emery, W.J., 1990. *Descriptive Physical Oceanography. An Introduction*, 5th Edition. Pergamon Press, New York, 320pp.
- Poisson, A., Chen, C.T.A., 1987. Why is there little anthropogenic CO₂ in the Antarctic Bottom water? *Deep-Sea Research I* 34, 1255–1275.
- Pollard, R.T., Griffiths, M.J., Cunningham, S.A., Read, J.F., Pérez, F.F., Ríos, A.F., 1996. Vivaldi 1991—A study of the formation, circulation and ventilation of Eastern North Atlantic Central Water. *Progress in Oceanography* 37, 167–192.
- Pérez, F.F., Álvarez, M., Ríos, A.F. Improvements on the back-calculation technique for estimating anthropogenic CO₂. *Deep-Sea Research*, submitted for publication.
- Pérez, F.F., Fraga, F., 1987a. The pH measurements in seawater on the NBS scale. *Marine Chemistry* 21, 315–327.
- Pérez, F.F., Fraga, F., 1987b. A precise and rapid analytical procedure for alkalinity determination. *Marine Chemistry* 21, 169–182.

- Pérez, F.F., Ríos, A.F., Fraga, F., Mouriño, C., 1985. Campaña “Galicia VI”. Datos básicos. Datos Informativos Instituto Investigaciones Pesqueras 11, 1–38.
- Rhein, M., Hinrichsen, H.H., 1993. Modification of mediterranean water in the Gulf of Cadiz, studied with hydrographic, nutrient and chlorofluoromethane data. *Deep-Sea Research I* 40, 267–291.
- Ríos, A.F., Pérez, F.F., 1999. Improvements in potentiometric determinations of CO₂ oceanic system using seawater sub-standards and CO₂ reference materials. *Ciencias Marinas* 25 (1), 31–49.
- Ríos, A.F., Pérez, F.F., Fraga, F., 1992. Water masses in the upper and middle North Atlantic Ocean east of the Azores. *Deep-Sea Research* 39, 645–658.
- Roos, M., Gravenhorst, G., 1984. The increase in oceanic carbon dioxide and the net CO₂ flux into the North Atlantic. *Journal of Geophysical Research* 89, 8181–8193.
- Sabine, C.L., Key, R.M., Johnson, K.M., Millero, F.J., Poisson, A., Sarmiento, J.L., Wallace, D.W.R., Winn, C.D., 1999. Anthropogenic CO₂ inventory of the Indian Ocean. *Global Biogeochemical Cycles* 13, 179–198.
- Sarmiento, J.L., Murnane, R., LeQuéré, C., 1995. Air-sea CO₂ transfer and the carbon budget of the North Atlantic. *Philosophical Transactions of the Royal Society of London* 348, 211–219.
- Saunders, P.M., 1982. Circulation in the eastern North Atlantic. *Journal of Marine Research* 40, 641–657.
- Schmitz, W.J., Jr., 1996. On the World Ocean Circulation: Volume I. Some Global Features/North Atlantic Circulation. Woods Hole Oceanographic Institution. Technical Report WHOI-96-03, 141pp.
- Siegenthaler, U., Sarmiento, J.L., 1993. Atmospheric carbon dioxide and the ocean. *Nature* 365, 119–125.
- Slater, D.R., Bryden, H.L., 2000. On the transport of Mediterranean outflow water, Report of the WOCE North Atlantic Workshop, WOCE Report 169/2000, WOCE International Project Office, Southampton, 106–107.
- Takahashi, T., Broecker, W.S., Langer, S., 1985. Redfield ratio based on chemical data from isopycnal surfaces. *Journal of Geophysical Research* 90, 6907–6924.
- Takahashi, T., Wanninkhof, R.H., Feely, R.A., Weiss, R.F., Chipman, D.W., Bates, N., Olafsson, J., Sabine, C., Sutherland, S.C., 1999. Net sea–air CO₂ flux over the global oceans: an improved estimate based on the sea–air *p*CO₂ difference. *Proceedings of the Second International Symposium CO₂ in the Oceans*, Tsukuba, CGER-1037-'99, pp. 9–15.
- UNESCO, 1986. Progress on oceanographic tables and standards 1983–1986. Work and Recommendations of UNESCO/SCOR/ICES/IAPSO Joint panel. UNESCO Technical Papers in Marine Science, 50p.
- Wanninkhof, R., Doney, S.C., Peng, T.H., Bullister, J.L., Lee, K., Feely, R.A., 1999. Comparison of methods to determine the anthropogenic CO₂ invasion into the Atlantic Ocean. *Tellus* 51B, 511–530.